Todo list

Extra long title which spans serveral lines and therefore has to be split manually and the vertical spacing has to be adjusted

My Name

My university

(Diploma/doctoral...) Thesis

Supervisor:

Prof. Dr. Supervisor

Supervisor's Department, University of ...

March 2013

Abstract

A novel method... It is based on...

Contents

List of Figures

List of Tables

Acknowledgements

First of all, I want to thank my supervisor...

I am very grateful for the guiding help of...

I am grateful to...

Chapter 1

Introduction

In the last few years...

Now my major contribution which is aaaaawesome...

Chapter 2

The Awesome Theory

The Large Hadron Collider (LHC) is a particle collider which is situated near Geneva, Switzerland and lies about 100 m below ground level.

Chapter 3

Fabrication of Nanodiamonds

"Diamond forms under high temperature and pressure conditions that exist only about 100 miles beneath the earths surface." (Homepage of the Gemological Institute of America Inc.) While this statement is true for natural gem diamonds, various methods exist to synthetically produce diamond for applications in industry and research. In this chapter, different fabrication methods of nanodiamondsare explained. The first two procedures described are the high-pressure, high-temperature method and the chemical vapor deposition are described. These are the most commonly used fabrication methods for laboratory-produced diamonds. The high-pressure, high-temperature (HPHT) process is similar to the natural growth process within earth and is widly used to synthetically produce diamonds for industry. Many measurements which are subject in this thesis are carried out on diamond produced with a CVD process. The third method mentioned is the wet-milling in a vibrational mill. The main focus of this thesis is on wet-milling nanodiamonds, which is a technique using chemical vapor deposition or HPHT diamond as starting material. It has to be stressed, that in contrast to the other methods described in this chapter, the wet-milling process is not a process to produce diamond itself, rather it serves to crush a bigger diamond into pieces of a desired size. For a more extensive list of diamond production processes refer for example to [**?**]. Aside from the diamond production processes, the technical details of the nanodiamondsused for this thesis will be mentioned.

3.1   High-Pressure High-Temperature Diamond

The HPHT process was the first process with which diamond was successfully synthesized (in 1879). Depending on the exact process, temperatures and pressures are needed of a few thousand degrees Celsius and 50 000 to a few 100 000, respectively [**?**]. Today, it is still widely used due to the relatively cheap production costs[**?**]. In this process, diamond is synthesized from graphite. For some forms of this method, a metallic solvent is added which lowers the needed pressures; the solvent causes the graphite to reach dissolve at lower pressures and temperatures, at the same time it causes the diamond to crystallize. The machine used for this kind of synthesis is a press. There exist several press designs, but they all provide a high temperature and a high pressure in their core. A disadvantage of the HPHT process is that it the reachable size of the produced diamonds is limited.

vorteile, n

mention in
NDs and I
NDs

3.2 Chemical Vapor Deposition Diamond

In contrast to the HPHT process, during the chemical vapor deposition process, diamond is grown from a vapor phase. The vapor is a mixture of hydrogen and methane, which acts as a carbon source. The vapor is energized to form a plasma by e.g. a microwaves. On the substrate surface, various processes occur, such as adsorption, desorption and diffusion. For crystals to form, initially seed crystals are necessary . There are several ways to coat a substrate with seed crystals. The easiest method is to spin-coat a substrate with small diamond crystals, of a size of a few nanometers, which is also the method exploited for the production processes described in this section. Growth on a substrate is easier, if the lattice constant of the substrate and the crystal to be grown are very similar. The lattice constant of iridium (0.384 nm[**?**]) is very similar to the lattice constant of diamond (0.356 nm[**?**]). Therefore, the diamonds were grown on a stratified substrate, consisting of iridium layers of 60 nm to 150 nm thickness grown onto an yttria-stabilized zirconia (YSZ) buffer layer, which in turn was grown on a silicon wafer.

To produce nanodiamonds, the growth process is stopped when the diamond grown on the seed crystals reaches the desired size.

One of the advantages of the CVD process is that silicon can be incorporated *in-situ*. This is achieved by the following process: silicon from the substrate edges is etched by the plasma and silicon atoms diffuse into the methane gas. These atoms are then build into the diamond lattice while growth.

In this thesis, two types of samples which were directly produced as nanodiamonds were investigated. The first batch (henceforth called CVD samples) were grown on detonation diamond seeds (produced by the company microdiamant, product Liquid Diamond monocrystalline, MSY 0-0.03 micron GAF) of a size smaller than 3 nm. For the growth process, 1% of methane was added to the hydrogen environment in the growth chamber. The growth process was performed with a pressure of 30 hPa for 30 min to 60 min, yielding nanodiamondsof a diameter of about 100 nm to 200 nm.

The other samples solely produced by a CVD process are nanodiamonds grown onto molecular analogs of diamond crystals. A subgroup of these molecular diamonds are called diamondoids and are carbon crystals based on the carbon cage molecule adamantane $C_{10}H_{16}$. The molecular diamonds used for this work are adamantane in cyclohexane, mercapto adamantane in cyclohexane, and cyclohexane. Each of these seed crystals was used in four different growth processes adding either 3% or 1% methane during growth to the hydrogen plasma and adding either silicon or silicon dioxide to form *in-situ* incorporated SiV centers.

3.3 Wet-Milled Nanodiamonds

Chapter 4

Confocal Setup

The key measurements of this thesis are fluorescence measurements of SiV centers in nanodiamonds. For this aim, a home-built confocal setup is used, which is described in this chapter.

The confocal setup serves to perform a series of measurements on fluorescence light: scanning the sample to find SiV centers, recording luminescence spectra of the aforementioned, determine the saturation count rate , and determine whether the emitter in question is a single emitter by performing photon autocorrelation measurements. The key components for these measurements are

- The confocal unit which serves to excite the emitters and collect the fluorescence light and move the sample while scanning.

- A grating spectrometer to investigate the spectral properties of the emitters. This is crucial to distinguish between SiV centers, other color centers and "dirt".

- A Hanbury Brown and Twiss (HBT) setup to investigate the single photon character. It is built up of two avalanche photo diodes (APDs) which also serve to scan the sample in order to find emitters on the sample surface; and to perform saturation measurements.

4.1 Confocal Unit

Figure 4.1 depicts a sketch of the confocal setup. Except for the laser and the sample stage, the whole setup is fixed to a vertical breadboard. This design allows for easy scanning and exchanging of the samples, without the need of gluing them to a vertical stage. The friction between the sample and the aluminum surface of the stage is sufficient that the sample does not move during scanning. If it is important that the sample has a a defined orientation, it is put inside of an aluminum angle. The stage is powered with two stepper motors () in the horizontal x and y directions. The objective is fixed to another stage which in turn is fixed to the vertical breadboard. In this way, the vertical z direction is implemented for focusing the laser light on the sample. Therefore, a three-axis scanning of the sample is implemented.

The bright red color at the left-hand side of the sketch represents the excitation beam path. The sample is excited with a continuous wave diode laser (Schäfter-Kirchhoff, 58FCM) which
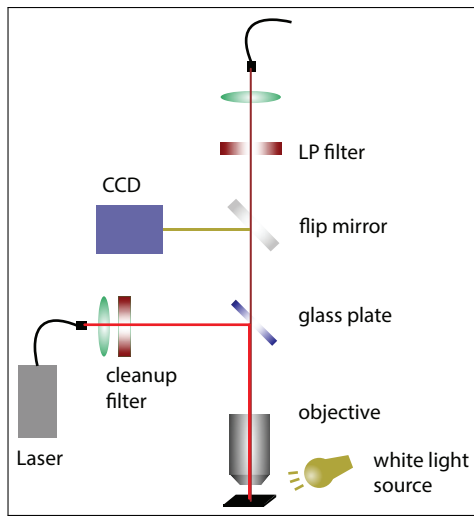
saturation
introduced
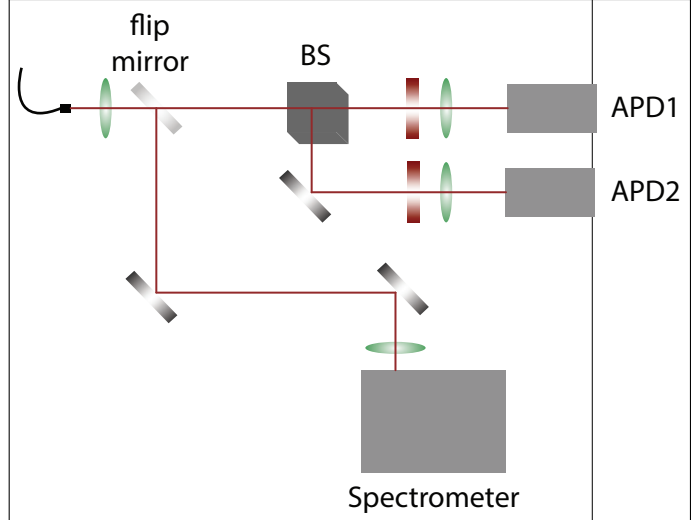
type

Figure 4.1: Confocal setup

Figure 4.2: HBT, spectrometer

emits at a wavelength of 660 nm. The outlet of the light is through a pigtail fiber, the light is outcoupled and collimated exploiting an aspheric lens. To suppress sideband emission from the laser, a bandpass filter with a window of 10 nm around a center of 660 nm is used. The excitation beam then hits a glass plate (fabricator Halle Germany) to be guided through a microscope objective and focused on the sample. The microscope objective is of the type Olympus, LMPlanFLN 100x and has a numerical aperture of 0.8. As the luminescence light from the emitter is in the same focus as the excitation laser light, it is effectively collected by the objective (hence "confocal setup").

The collected light then follows the detection beam path depicted in a dark red color in Figure 4.1. Both the excitation light reflected from the sample surface and the fluorescence light pass through the glass plate. In the usual useage, the flip mirror just after the beamsplitter is lowered, allowing the light coming from the sample to move on towards a single mode fiber. In front of the single mode fiber there is a longpass filter of a cutoff wavelength of 710 nm or 720 nm to filter out the residual excitation light and also ambient light. The fluorescence light is fed into a single-mode fiber (Thorlabs SM600) with an aspheric lens. The single-mode fiber serves two purpuses: First, to connect the confocal microscope with the HBT setup and the spectrometer. Second, its about 4.3 μm diameter serves as a pinhole to ensure optimal resolution. In the direction of the optical axis the resolution amounts to , in the plane of the sample it is .

According to the experimental necessities, instead of the mentioned glass plate a dichroic mirror () can be employed. A dichroic mirror spectrally separates the incident light by transmitting and reflecting it as a function of the wavelength. Hence, excitation light is separated from fluorescence light. The glass plate features a high transmission of 90%and therefore a high collection efficiency of fluorescence light, whereas the dichroic mirror allows for a higher excitation intensity using the same excitation laser. However, a high excitation intensity may cause permanent fluorescence intermittence of the SiV centers (for further detail, refer to). In general, if a high excitation is necessary, for instance for saturation measurements , the dichroic mirror is used; otherwise, the glass plate is used to collect as much fluorescence light as possible.

4.2 Optical Imaging of The Sample Surface

Another feature of the setup is that it is possible to have a look at the sample surface before starting the fluorescence measurements. For this purpose, the sample is illuminated with white light from a halogen lamp and the flip mirror after the glass plate is brought into an upright position to guide the light onto a CCD camera (). The scattered light from the sample surface is collected by the objective and the surface is shown on the CCD image. Nanodiamonds and other features on the substrate are visible, the resolution of this setup is limited by . However, it suffices to find the markers of a dimension of 10 μm which are milled into some substrates and to recognize characteristic patterns of the coated nanodiamonds.

4.3 Spectrometer

Figure 4.2 displays the detector part of the setup. The fluorescence light in the fiber coming from the confocal unit is outcoupled with an aspheric lens. A flip mirror is employed to direct the light either to a grating spectrometer or the HBT setup.

As mentioned before, the fluorescence light from the SiV centers is investigated with the grating spectrometer to evaluate the source of the fluorescence light by comparing the measured spectrum to typical spectra from known sources. The spectrometer is a Princeton Instruments Acton2500i spectrometer. The incident beam passes through an entrance slit, is then scattered on the grating where the light is spectrally divided and finally hits a detector, imaging the entrance slit on the detector surface. The employed detector is a CCD camera ()which is cooled with liquid nitrogen for noise reduction. It enables detection of light up to a wavelength of 1000 nm. The spectrometer features three gratings: 600 grooves/mm, 1200 grooves/mm, and 1800 grooves/mm. With a step-and-glue function of the spectrometer software (WinSpec) it is possible, to record several spectra over a wide wavelength range which are then stiched together. It is therefore possible to combine a larger wavelength range with a higher resolution. For most measurements the grating with 600 grooves/mm was used. The resolution of the spectrometer using the 600 grooves mm^{-1} is xxas stated by the manufacturer. This resolution suffices for most of the measurements mentioned in this work.

4.4 Hanbury Brown and Twiss Setup

An Hanbury Brown and Twiss setup serves to record the photon autocorrelation function ($g^{(2)}$ function) of an emitter. In the photon number representation, it is defined as follows:

$$g^{(2)}(0) = \frac{\langle N(t)N(t+\tau)\rangle}{\langle N(t)\rangle^2}.$$

Here, $N(t)$ denotes the photon at a certain time t, $N(t+\tau)$ denotes the photon at a time interval τ later than t. The angular brackets $\langle\rangle$ denote the temporal averaging. In this work, the $g^{(2)}$ function is used to make statements about whether the emitter emits single photon and is therefore one single emitter. The physical explanation is that if the emitter is a single emitter and emits at a time t, the next time any photon is recorded is at time $t+\tau$. For a time interval close to zero, the value of the $g^{(2)}$ function must ideally approach zero or at

least be smaller than 0.5 if only a single emitter is present: The denominator is zero, because $N(t + \tau)(\tau = 0) = 0$ due to only one photon, namely $N(t)$ being present. If two photons are emitted at the same time (time delay zero), the $g^{(2)}$ function yields $g^{(2)}(0) = 0.5$. (For a detailed explanation of the $g^{(2)}$ function read [**?**])

The principle of the HBT setup is to evaluate the time delay between two consecutive photons. A sketch of the HBT setup is shown in Figure 4.2. The photons are detected with avalanche photo diodes of the type PicoQuant τ-SPAD 100 . These avalanche photo diodes have a nominal detection efficiency of up to 70% at the optimal wavelength of about 670 nm, a dark count rate of under 100 cps, and a dead time to avoid afterpulsing of about 70 ns. In the ideal case, one APD would be enough to measure the time delay between two consecutive photons. However, the second of two consecutive photons could hit the detector during its dead time. To circumvent this problem, two APDs are employed and the detection beam is split with a non-polarizing 50:50 beamsplitter cube (). Each beam then passes through a bandpass filter and is focused on the avalanche photo diode with a lens . As the beam path is slightly different for each APD, a small optical path difference is introduced, however, this difference only results in an offset of the $g^{(2)}$ function and does not alter the physical nature of the result. The bandpass filters serve two reasons: First, they limit optical crosstalk between the avalanche photo diodes. The process of detection of an avalanche photo diode produces light due to recombination of charge carriers. Crosstalk between two avalanche photo diodes occurs, if one of the photons produced by one avalanche photo diode escapes and is detected in the other one [**?**]. Secondly the bandpass filters serve to reduce background during the $g^{(2)}$ measurement process or to spectrally divide emission from several emitters. Therefore, it is possible to find single emitters, which are not spatially seperated enough to be seperated with the spatial resolution of the setup, but can be spectrally seperated if their ZPLs are apart enough that respective bandpass filters can be used to only investigate light from one ZPL.

When the APD fires, it outputs a digital TTL (transistor-transisor logic) signal. The arrival times of the signals are recorded with a time tagging module (). One list of arrival times (so-called time tags) is recorded for each APD and stored as raw data. The time uncertainty of the photon detection process introduces variations of the digital signal's instant from its ideal position in time and therefore introduces affects the time tags and with them the $g^{(2)}$ function. A discussion of the impact of timing jitter will be given in **??**. Those lists are to determine the $g^{(2)}$ function and therefore determine whether the detected light stems from a single photon source. To get a single array of arrival times of the photons, which can then be binned to obtain the $g^{(2)}$ function, the arrays of the two APDs have to be correlated. For that, the time difference between each entry in one array and all consecutive time tags in the other array are determined and stored according a binning defined by the user. After normalizing and fitting these data, statements about whether the emitter is a single emitter can be made.
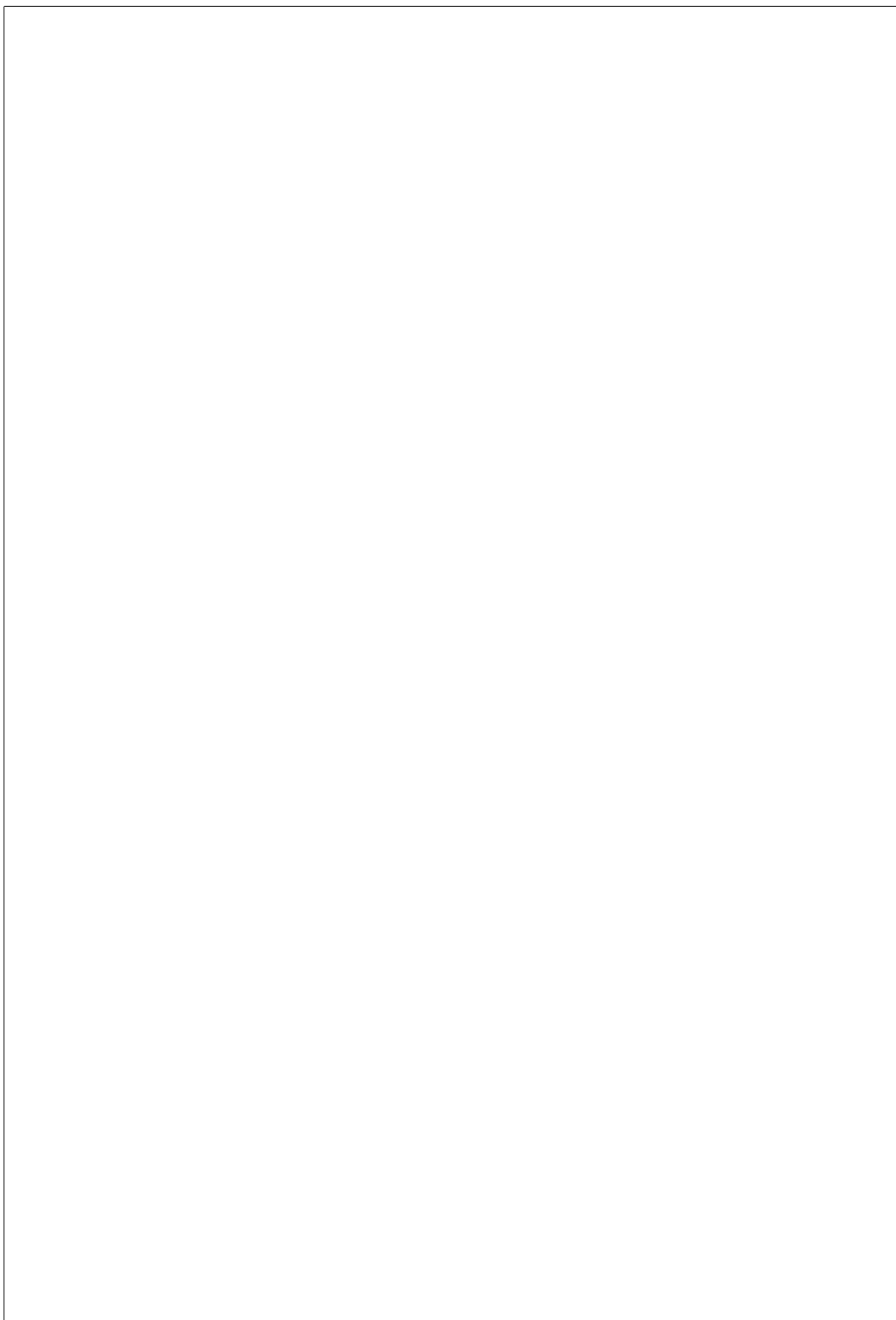
Chapter 5

discussion

Chapter 6

Conclusion

In conclusion...

Appendix A

Text of Minor Interest

Some data

Bibliography

Index

$g^{(2)}$ function, 7

Hanbury Brown and Twiss, 5
Hanbury Brown and Twiss setup, **7**

LHC, 2

photon autocorrelation function, 7